Auger cascades in aluminum*

Eugene J. McGuire
Sandia Laboratories, Albuquerque, New Mexico 87115
(Received 2 December 1974)

Transition-rate expressions are developed to analyze the Auger cascade leading to multiply charged ions following inner-shell vacancy production. In general, our aim is to predict the intensity and spectral distribution of the soft x-ray emission occurring at the termination of the Auger cascade, to determine when and if there can be an inner-shell population inversion, and at what pumping level one will obtain amplified spontaneous emission. Aluminum is examined in detail starting with an initial K-shell vacancy, and it is found that there can be significant amplified spontaneous emission in the 160–170-Å region providing one has a hard x-ray flux of about 10^{11} W/cm^2 at energies greater than the Al K-shell binding energy. It is hypothesized that the recent observations of Jaegle *et al.*, indicating gain at 117.4 Å in a two-plasma experiment, can be accounted for via x-ray coupling between the plasmas. An experiment to check the hypothesis is advanced.

I. INTRODUCTION

When an inner-shell vacancy is created in an atom, the vacancy decays by Auger and radiative processes.[1-3] In the first step of the Auger process, the single vacancy decay leads to two vacancies in shells with higher principal quantum numbers. In many instances, the double vacancy state can undergo Auger transitions, etc. This I will refer to as an Auger cascade. The cascade will terminate when energetics, selection rules, or the absence of outer electrons forbids further Auger decay. At the termination of the Auger process, the resultant ions will not necessarily be in their ground state. They pass to the ground state by radiative transitions or collisions with other particles. There may be significant population inversions. In many instances, the Auger transition rate is orders of magnitude greater than the radiative transition rate, and except for K-shell fluorescence at intermediate and high Z, and L-shell fluorescence at high Z, one may neglect radiative transitions until the Auger cascade has terminated. Almost all the theoretical and experimental work on inner-shell vacancy decay has been limited to the first step in the decay process (i.e., measurements of fluorescence yields and Auger electron spectra).[1-5] However, Krause and Carlson[6] have examined one aspect of the Auger cascade, the distribution of final charge states. Counting ions with a mass spectrometer (with the long transit times involved) precludes a determination of the ion term distribution after the Auger cascade but prior to radiative decay. Yet, at this stage, it should be possible to determine the term distribution via the characteristic soft-x-ray emission (signature) of the ion. The soft-x-ray signature is, of course, contained in the total emission spectrum of the recombining ions, and separating the two can be a difficult experimental problem.

Up to the present, theory has been of little help. A theory of Auger decay should be capable of predicting the population of final states in the Auger cascade, and predicting relative radiative transition intensities from these final states (i.e., it should predict the characteristic x-ray signature). If reliable, it should permit the separation of the ion recombination spectrum from the soft-x-ray signature. The reason no theoretical information is available is that such Auger transition rates are between terms of multivacancy ions. Recently, I have obtained such multivacancy Auger transition-rate expressions.[3] However, the expressions were obtained in terms of quantum numbers which, while they simplified the resultant expressions, were not the physically relevant quantum numbers. For studies of multiplet effects in transition elements[7] and rare earths,[8] the expressions were recast so that they involved the physically relevant quantum numbers. In Sec. II of this paper, we obtain transformed expressions relevant to Auger cascades in L-S coupling.

The motivation for this study is the possibility that Auger cascades can lead to inner-shell population inversions of sufficient magnitude to produce soft-x-ray amplified spontaneous emission. I have recently proposed such a scheme, and used Na^+ as an example.[9] The Auger cascade for such a system is simple; it is a classic K-LL Auger decay. One factor contributing to its inefficiency is that it uses the weak K-$L_1L_{23}(^3P)$ transition rather than the strong K-$L_{23}L_{23}(^1D)$ transition to populate the upper level in the inner-shell inversion. One expects better efficiency when the upper level arises from $L_{23}L_{23}(^1D)$. Al is such a system. However, the Auger cascade now involves at least two steps, and partially filled shells enter from the beginning. Al is also interesting in that Jaegle *et*

al.[10] have reported a possible inner-shell inversion in Al^{+3}, and Al^{+3} is the ion terminating the K-$L_{23}L_{23}(^1D)$ Auger cascade. Valero[11] reports that the experiment of Jaegle *et al.*[10] can be accounted for by strong self-absorption of some Al^{+3} emission, and weak self-absorption of other emission lines, leading to the appearance of enhanced emission in the weakly self-absorbed lines. The possibility that the Auger cascade following K-shell vacancy production in Al may play a role in the observations is discussed in Sec. IV.

II. TRANSITION RATES IN L-S COUPLING FOR AUGER CASCADES

To determine the Auger transition rate between ionic terms, one must have a reasonable prescription for describing the terms. For example, in a $2s$-$3p$, $3d$ Auger transition in an ion with a single $3s$ vacancy, and partially filled $2s$, $3p$, $3d$, and N shells, a reasonable prescription would be to add a ^2S from the $2s$- to the $2p$-shell quantum numbers, add the ^2S from the $3s$ shell to the resultant, separately add the $3p$ and $3d$ quantum numbers, add this resultant to the previous resultant, then add the quantum numbers from the partially filled N shell to obtain total quantum numbers. It seems doubtful that any experiment could resolve a term of this type. In the interest of simplicity, we describe such a term by adding ^2S from the $2s$ to the $2p$ shell, adding the ^2S from the $3s$ to the N-shell quantum numbers, and adding the resultant to a resultant obtained by adding the $3p$- and $3d$-shell quantum numbers, then adding this to the inner-shell resultant. That is, the most general transition rate we obtain will be of the form

$$[(n_1l_1)^{m+1}L_1S_1, P_{R_1}Q_{R_1}; D_1D_4][(n_3l_3)^nL_3S_3, (n_4l_4)^pL_4S_4; A_2B_2, P_{R_2}Q_{R_2}; D_2D_5]D_3D_6$$
$$\rightarrow [(n_1l_1)^mP_1Q_1, P_{R_1}Q_{R_1}; C_1C_3][(n_3l_3)^{n+1}P_3Q_3, (n_4l_4)^{p+1}P_4Q_4; A_1B_1, P_{R_2}Q_{R_2}; C_2C_4]PQ.$$

The Auger transition rate averaged over initial terms for the transition

$$[(n_1l_1)^{m+1}L_1S_1, l_2\tfrac{1}{2}; XY][(n_3l_3)^nL_3S_3, (n_4l_4)^pL_4S_4; A_2B_2, P_RQ_R; A_4B_4]PQ$$
$$\rightarrow [(n_3l_3)^{n+1}P_3Q_3, (n_4l_4)^{p+1}P_4Q_4; A_1B_1, (n_1l_1)^mP_1Q_1; A_3B_3, P_RQ_R; PQ]$$

was found to be[6]

$$W_{if}(7) = 2\pi \frac{(2P_3+1)(2Q_3+1)(2P_4+1)(2Q_4+1)(2P+1)(2Q+1)}{(2P_R+1)(2Q_R+1)(2L_3+1)(2S_3+1)(2L_4+1)(2S_4+1)}$$
$$\times \prod_{i=1}^{4}(2l_i+1)\sum_{X,Y}(2X+1)(2Y+1)\sum_{A_i,B_i}\prod_{i=1}^{4}(2A_i+1)(2B_i+1)$$
$$\times\left|\sum_{f,g}(-1)^f(2f+1)(2g+1)I(KK'fg)F_1\begin{Bmatrix}A_2 & A_3 & X\\ P & A_4 & P_R\end{Bmatrix}\begin{Bmatrix}P_1 & g & X\\ l_2 & L_1 & l_1\end{Bmatrix}\begin{Bmatrix}P_1 & g & X\\ A_2 & A_3 & A_1\end{Bmatrix}\begin{Bmatrix}A_1 & P_4 & P_3\\ A_2 & L_4 & L_3\\ g & l_4 & l_3\end{Bmatrix}\right.$$
$$\left.\times\begin{Bmatrix}B_2 & B_3 & Y\\ Q & B_4 & Q_R\end{Bmatrix}\begin{Bmatrix}Q_1 & f & Y\\ \frac{1}{2} & S_1 & \frac{1}{2}\end{Bmatrix}\begin{Bmatrix}Q_1 & f & Y\\ B_2 & B_3 & B_1\end{Bmatrix}\begin{Bmatrix}B_1 & Q_4 & Q_3\\ B_2 & S_4 & S_3\\ f & \frac{1}{2} & \frac{1}{2}\end{Bmatrix}\right|^2, \tag{1}$$

where

$$I(KK'fg) = \sum_K D(K)\begin{Bmatrix}l_1 & l_3 & K\\ l_4 & l_2 & g\end{Bmatrix} + (-1)^{f-g}\sum_{K'}E(K')\begin{pmatrix}l_1 & l_4 & K'\\ l_3 & l_2 & g\end{pmatrix},$$

$$D(K) = R_K(l_1l_2l_3l_4)\begin{pmatrix}l_1 & K & l_3\\ 0 & 0 & 0\end{pmatrix}\begin{pmatrix}l_2 & K & l_4\\ 0 & 0 & 0\end{pmatrix},\quad E(K) = R_K(l_1l_2l_4l_3)\begin{pmatrix}l_1 & K & l_4\\ 0 & 0 & 0\end{pmatrix}\begin{pmatrix}l_2 & K & l_3\\ 0 & 0 & 0\end{pmatrix},$$

$$R_K(l_1l_2l_3l_4) = \iint dr_1\,dr_2\,\Psi_{l_1}(r_1)\Psi_{l_2}(r_2)\frac{(r_<)^K}{(r_>)^{K+1}}\Psi_{l_3}(r_1)\Psi_{l_4}(r_2).$$

In the above l_2 is the angular momentum quantum number of a continuum orbital. The terms in parentheses

are 3-j symbols, and those in brackets are 6-j and 9-j symbols.[15] The quantity F_1 is given by

$$F_1=[(m+1)(n+1)(p+1)]^{1/2}(l_1^{m+1}\alpha_1 L_1 S_1 [l_1^m \beta_1 P_1 Q_1)(l_3^{n+1}\beta_3 P_3 Q_3 [l_3^n \alpha_3 L_3 S_3)(l_4^{p+1}\beta_4 P_4 Q_4 [l_4^p \alpha_4 L_4 S_4),$$

where here the terms in parentheses are fractional parentage coefficients.[16]

When both electrons come from the same shell (i.e., $n_3 l_3 = n_4 l_4$, one obtains the appropriate transition rate by substituting into Eq. (1)

$$[(2P_3+1)(2Q_3+1)]^{1/2}F_1 \to F_3=\tfrac{1}{2}[(m+1)(n+1)(n+2)]^{1/2}(l_1^{m+1}\alpha_1 L_1 S_1 [l_1^m \beta_1 P_1 Q_1)$$
$$\times \sum_{\beta_3' P_3' Q_3'} [(2P_3'+1)(2Q_3'+1)]^{1/2}(l_3^{n+2}\beta_3 P_3 Q_3 [l_3^{n+1}\beta_3' P_3' Q_3')(l_3^{n+1}\beta_3' P_3' Q_3' [l_3^n \alpha_3 L_3 S_3),$$

$$l_4 \to l_3, \quad P_3 Q_3 \to P_3' Q_3', \quad A_1 B_1 \to P_3 Q_3, \quad A_3 B_3 \to A_1 B_1, \quad A_4 B_4 \to A_2 B_2$$

and $L_4 = S_4 = 0$. Then to transform the equivalent electron transition rate to one involving the relevant quantum numbers, one merely makes the above substitutions in the transformed inequivalent expression. After transforming Eq. (1), one must multiply by

$$(2L_1+1)(2S_1+1)(2L_3+1)(2S_3+1)(2L_4+1)(2S_4+1)(2P_R+1)(2Q_R+1)/(2D_3+1)(2D_6+1)$$

to convert the transition rate from one averaged over initial states to one appropriate to the initial term.

In an earlier paper on multiplet structure[7] we obtained the necessary expressions by a transformation of Clebsch-Gordan coefficients used in deriving Eq. (1). This is unsatisfactory because unless one knows the original choice of Clebsch-Gordan coefficients, the transformation is correct only up to a phase factor, and an incorrect phase factor can lead to a physically incorrect result. Since Eq. (1) does not indicate the original choice of Clebsch-Gordan coefficients, and since the transition rate should be independent of coupling, it is clear one should obtain transformed expressions directly from Eq. (1).

For the transition

$$[(l_1)^{m+1}L_1 S_1, P_{R_1}Q_{R_1}; D_1 D_4][(l_3)^n L_3 S_3, (l_4)^p L_4 S_4; A_2 B_2, P_{R_2}Q_{R_2}; D_2 D_5]D_3 D_6$$
$$\to [(l_1)^m P_1 Q_1, P_{R_1}Q_{R_1}; C_1 C_3][(l_3)^{n+1}P_3 Q_3, (l_4)^{p+1}P_4 Q_4; A_1 B_1, P_{R_2}Q_{R_2}; C_2 C_4]PQ,$$

the Auger transition rate is

$$W_{if}(a)=2\pi(2L_1+1)(2S_1+1)(2P_3+1)(2Q_3+1)(2P_4+1)(2Q_4+1)(2P+1)(2Q+1)$$
$$\times \prod_{i=1}^{4}(2l_i+1)(F_1)^2(2A_1+1)(2B_1+1)(2C_1+1)(2D_1+1)(2A_2+1)(2B_2+1)(2C_2+1)$$
$$\times (2D_2+1)(2D_4+1)(2D_5+1)(2C_3+1)(2C_4+1)\begin{Bmatrix} l_1 & C_1 & D_1 \\ P_{R_1} & L_1 & P_1 \end{Bmatrix}^2 \begin{Bmatrix} \frac{1}{2} & C_3 & D_4 \\ Q_{R_1} & S_1 & Q_1 \end{Bmatrix}^2$$
$$\times \left| \sum_{f,g} (-1)^f (2f+1)(2g+1) I(KK'fg) \begin{Bmatrix} g & D_2 & C_2 \\ P_{R_2} & A_1 & A_2 \end{Bmatrix} \begin{Bmatrix} f & D_5 & C_4 \\ Q_{R_2} & B_1 & B_2 \end{Bmatrix} \right.$$
$$\left. \times \begin{Bmatrix} g & C_2 & D_2 \\ l_2 & P & D_3 \\ l_1 & C_1 & D_1 \end{Bmatrix} \begin{Bmatrix} A_1 & P_4 & P_3 \\ A_2 & L_4 & L_3 \\ g & l_4 & l_3 \end{Bmatrix} \begin{Bmatrix} f & C_4 & D_5 \\ \frac{1}{2} & Q & D_6 \\ \frac{1}{2} & C_3 & D_4 \end{Bmatrix} \begin{Bmatrix} B_1 & Q_4 & Q_3 \\ B_2 & S_4 & S_3 \\ f & \frac{1}{2} & \frac{1}{2} \end{Bmatrix} \right|^2 . \tag{2}$$

The derivations of Eqs. (2) and (5) clearly involve extensive algebraic manipulation. In Eqs. (3a)–(3e) are shown some steps in the manipulation. We begin with

$$I=\sum_{x, A_3, A_4}(2x+1)(2A_3+1)(2A_4+1)\left| \begin{Bmatrix} A_2 & A_3 & x \\ P & A_4 & P_R \end{Bmatrix} \begin{Bmatrix} P_1 & g & x \\ l_2 & L_1 & l_1 \end{Bmatrix} \begin{Bmatrix} P_1 & g & x \\ A_2 & A_3 & A_1 \end{Bmatrix} \cdots \right|^2 \tag{3a}$$

and seek to insert the triads (A_2, P_{R_2}, D_2) and (A_1, P_{R_2}, C_2). A difficulty is that Eq. (1) or Eq. (3a) contains

P_R, not P_{R_1} and P_{R_2}. This is remedied by using

$$(2P_R+1)\sum_t (2t+1)\begin{Bmatrix} P_{R_1} & P_{R_2} & P_R \\ A_2 & A_4 & t \end{Bmatrix}^2 = 1, \tag{3b}$$

so that

$$I=(2P_R+1)\sum_{x,\,t,\,A_3A_4}(2x+1)(2t+1)(2A_3+1)(2A_4+1)\left|\begin{Bmatrix} P_{R_1} & P_{R_2} & P_R \\ A_2 & A_4 & t \end{Bmatrix}\begin{Bmatrix} A_2 & A_3 & x \\ P & A_4 & P_R \end{Bmatrix}\begin{Bmatrix} P_1 & g & x \\ l_2 & L_1 & l_1 \end{Bmatrix}\begin{Bmatrix} P_1 & g & x \\ A_2 & A_3 & A_1 \end{Bmatrix}\cdots\right|^2. \tag{3c}$$

If we call the term in absolute value I_1 and apply the Biedenharn-Elliott[12] (BE) identity to the first two terms, then apply the BE identity to a resultant term and the third term in I, we have, on dropping irrelevant phase factors

$$I_1=\sum_{Z_1Z_2}(-1)^{Z_1+Z_2+g}(2Z_1+1)(2Z_2+1)$$
$$\times\begin{Bmatrix} Z_1 & P_1 & Z_2 \\ g & t & x \end{Bmatrix}\begin{Bmatrix} g & t & Z_2 \\ P_{R_2} & A_1 & A_2 \end{Bmatrix}\begin{Bmatrix} P_{R_2} & A_1 & Z_2 \\ P_1 & Z_1 & A_3 \end{Bmatrix}\begin{Bmatrix} x & t & Z_1 \\ P_{R_1} & P & A_4 \end{Bmatrix}\begin{Bmatrix} P_{R_1} & P & Z_1 & P_1 & g & x \\ A_3 & P_{R_2} & P_R & l_2 & L_1 & l_1 \end{Bmatrix}. \tag{3d}$$

With I_1 in this form we can sum over A_4, so that

$$I=(2P_R+1)\sum_{x,\,A_3,\,t,\,Z_1}(2t+1)(2x+1)(2A_3+1)(2Z_1+1)$$
$$\times\left|\sum_{Z_2}(-1)^{g+Z_2}(2Z_2+1)\begin{Bmatrix} Z_1 & P_1 & Z_2 \\ g & t & x \end{Bmatrix}\begin{Bmatrix} g & t & Z_2 \\ P_{R_2} & A_1 & A_2 \end{Bmatrix}\begin{Bmatrix} P_{R_2} & A_1 & Z_2 \\ P & Z_1 & A_3 \end{Bmatrix}\begin{Bmatrix} P_{R_1} & P & Z_1 \\ A_3 & P_{R_2} & P_R \end{Bmatrix}\begin{Bmatrix} P_1 & g & x \\ l_2 & L_1 & l_1 \end{Bmatrix}\right|^2.$$

At this point with $t\to D_2$, $Z_2\to C_2$, we have introduced the two triads into the transition rate expression. The other triads (L_1, P_{R_1}, D_1), (P_1, P_{R_1}, C_1), (D_1, D_2, D_3), and (C_1, C_2, P) are introduced in a similar fashion leading to an expression involving a 9-j symbol containing the irrelevant quantum numbers A_3 and P_R. These are summed over, leading to Eq. (2).

Using the substitutions mentioned earlier, we find the Auger rate for the transition

$$[(l_1)^{m+1}L_1S_1, P_{R_1}Q_{R_1}; D_1D_4][(l_3)^nL_3S_3, P_{R_2}Q_{R_2}; D_2D_5]D_3D_6 \to [(l_1)^mP_1Q_1, P_{R_1}Q_{R_1}; C_1C_3][(l_3)^{n+2}P_3Q_3, P_{R_2}Q_{R_2}; C_2C_4]PQ$$

is given by

$$W_{if}(b)=2\pi(2L_1+1)(2S_1+1)(2P_3+1)(2Q_3+1)(2P+1)(2Q+1)(2l_3+1)$$
$$\times\prod_{i=1}^{3}(2l_i+1)(2C_1+1)(2D_1+1)(2C_2+1)(2D_2+1)(2C_3+1)(2C_4+1)$$
$$\times(2D_4+1)(2D_5+1)\begin{Bmatrix} l_1 & C_1 & D_1 \\ P_{R_1} & L_1 & P_1 \end{Bmatrix}^2\begin{Bmatrix} \frac{1}{2} & C_3 & D_4 \\ Q_{R_1} & S_1 & Q_1 \end{Bmatrix}^2$$
$$\times\left|F_3(-1)^{2(Q_3'+P_3')}\sum_{f,g}(-1)^g(2f+1)(2g+1)I(KK'fg)\begin{Bmatrix} g & D_2 & C_2 \\ P_{R_2} & P_3 & L_3 \end{Bmatrix}\begin{Bmatrix} l_3 & g & l_3 \\ P_3 & P_3' & L_3 \end{Bmatrix}\right.$$
$$\left.\times\begin{Bmatrix} g & C_2 & D_2 \\ l_2 & P & D_3 \\ l_1 & C_1 & D_1 \end{Bmatrix}\begin{Bmatrix} f & D_5 & C_4 \\ Q_{R_2} & Q_3 & S_3 \end{Bmatrix}\begin{Bmatrix} \frac{1}{2} & f & \frac{1}{2} \\ Q_3 & Q_3' & S_3 \end{Bmatrix}\begin{Bmatrix} f & C_4 & D_5 \\ \frac{1}{2} & Q & D_6 \\ \frac{1}{2} & C_3 & D_4 \end{Bmatrix}\right|^2. \tag{4}$$

In the limit that $P_{R_1}Q_{R_1}=P_{R_2}Q_{R_2}={}^1S$, and $P_1Q_1=L_3S_3={}^1S$ corresponding to filled shells Eq. (2) reduces to

Eq. (5) of Ref. 7. In the limit that $P_{R_1}Q_{R_1}=P_{R_2}Q_{R_2}={}^1S$, one can reduce Eq. (4), with some algebraic manipulation, to Eq. (22) of Ref. 7. Thereby, we obtain the transition rate expressions of Ref. 7 without using arguments involving Clebsch-Gordan coefficients.

Finally, for the transition

$$[(l_1)^{m+1}L_1S_1,(l_3)^nL_3S_3;D_1D_4][(l_4)^pL_4S_4,P_RQ_R;D_2D_5]D_3D_6\rightarrow[(l_1)^mP_1Q_1,(l_3)^{n+1}P_3Q_3;C_1C_3]\times[(l_4)^{p+1}P_4Q_4,P_RQ_R;C_2C_4]PQ\,,$$

we find the expression

$$W_{if}(c)=2\pi(2L_1+1)(2S_1+1)(2P_3+1)(2Q_3+1)(2P_4+1)(2Q_4+1)(2P+1)(2Q+1)\times\prod_{i=1}^{4}(2l_i+1)F_1^2\,(2C_1+1)(2D_1+1)(2C_2+1)(2D_2+1)(2C_3+1)(2C_4+1)\times(2D_4+1)(2D_5+1)\begin{Bmatrix}P_R & P_4 & C_2\\ l_4 & D_2 & L_4\end{Bmatrix}^2\begin{Bmatrix}Q_R & Q_4 & C_4\\ \frac{1}{2} & D_5 & S_4\end{Bmatrix}^2\times\left|\sum_f(-1)^f(2f+1)(2g+1)I(KK'fg)\sum_{\mu,\nu}(-1)^{\mu+\nu}(2\mu+1)(2\nu+1)\begin{Bmatrix}l_3 & l_1 & \mu\\ l_2 & l_4 & g\end{Bmatrix}\begin{Bmatrix}\frac{1}{2} & \frac{1}{2} & \nu\\ \frac{1}{2} & \frac{1}{2} & f\end{Bmatrix}\times\begin{Bmatrix}l_3 & l_1 & \mu\\ P_3 & P_1 & C_1\\ L_3 & L_1 & D_1\end{Bmatrix}\begin{Bmatrix}l_2 & l_4 & \mu\\ D_3 & D_2 & D_1\\ P & C_2 & C_1\end{Bmatrix}\begin{Bmatrix}\frac{1}{2} & \frac{1}{2} & \nu\\ Q_3 & Q_1 & C_3\\ S_3 & S_1 & D_4\end{Bmatrix}\begin{Bmatrix}\frac{1}{2} & \frac{1}{2} & \nu\\ D_6 & D_5 & D_4\\ Q & C_4 & C_3\end{Bmatrix}\right|^2. \tag{5}$$

Readers knowledgeable in the theory of angular momentum will recognize that the sums on μ and ν can be written as 15-j symbols of the fourth kind.[13] However, for practical purposes we have left Eq. (5) in its inelegant form.

III. AUGER CASCADE IN ALUMINUM

Before calculating the Auger transition rates, one needs a reasonable energy-level diagram for the element in question. In Fig. 1 we show such a diagram for Al. The solid lines are obtained from the ESCA tabulation[14] and Moore's tables,[15] supplemented by measurements of Abouaf[16] (in the 90–100-eV range in Al^{+2}), and the fact (based on observations on Al^{+1}, Al^{+3}, and Al^{+4}) that the $2s$-$2p$ energy difference is about 44 eV. The notation used is that suggested by Larkins,[17] that a vacancy be designated by $[nl]$ and an electron by (nl), so that $(1s)^2(2s)^2(2p)^5(3s)^0(3p)^0(3d)^1$ is written as $[2p][3s]^2[3p](3d)$. The zero of energy in Fig. 1 is the ground state of neutral Al. We have no experimental data allowing us to locate the states with double L-shell vacancies (i.e., simultaneous measurement of K-LL and K-LM energies). Thus, in Fig. 1 these states are designated by dashed lines. For the Al^{+2} double L-shell vacancies we used the ESCA K-shell ionization energy and the K-LL energy differences calculated by Shirley.[18] For Al^{+3} we used the approximation that $E([2s]^2)-E([2s]^2[3p])$ in Al should be approximately equal to $E([3p]^2)-E([3p]^3)$ in P. This leads to an energy difference of 30 eV; this value is approximately the $E([2p][3s])-E([2p][3s][3p])$ value from known levels in Al. We also used the value 10 eV for the $(3s)-(3p)$ energy difference in Al^{+3}.

The energy-level diagram is important in determining whether Coster-Kronig transitions are allowed. For example, one could have $[2s]^2\,{}^2P$ in Al^{+2} cascade to a term of $[2s][2p][{}^1P][3s]$ in Al^{+3}, with a further cascade to a term of $[2p]^2[3s][3p]$ in Al^{+4}. The latter configuration would decay radiatively to the ground state of Al^{+4} by a $3s$-$2p$ transition. Such a possibility depends on the location of the energy levels involved, and Fig. 1 is not sufficiently accurate to decide this. Further, in the lowest approximation, we are using the assumption that double Auger transitions can be neglected, that is we are neglecting the possibility of $[2p]^2\rightarrow[2s][3s][3p]$ transitions which are energetically allowed in Fig. 1. Thus, in the lowest approximation, the $[2p]^2$ configurations cannot decay by Coster-Kronig processes, and will have relatively long lifetimes ($\Gamma\ll 1$ eV). However, it is well established in Auger spectroscopy[19] that for low-Z elements $[2p]^2\,{}^1S$ contains a significant admixture of $[2s]^2\,{}^1S$ via configuration interaction, even though the levels are many tens of eV apart. Since, in Al, $[2s]^2\,{}^2P$ can decay to $[2s][3s]^2$ and $[2s][3s][3p]$, and since $[2p]^2[{}^1S]^2P$ and

$[2p]^2[\,^1D]^2P$ can have configuration interaction with $[2s]^2\,^2P$, in a more sophisticated treatment, including configuration interaction, the $[2s][3s]^2\,^{1,3}P^0$ terms can be populated by cascades from $[2p]^2[\,^1S]^2P$ and $[2p]^2[\,^1D]^2P$. We shall return to this point later in this section.

The relevant transition rates for Auger cascades in Al were calculated using Eqs. (2)–(5). The formal expressions are simple (they always involve at least one s electron), but there are so many that we do not list them. Instead, we list the ion levels in Al^{+2} and their lifetimes, the levels to which they decay in Al^{+3} and their lifetimes, and the percent of $1s$ vacancies that reach the final state term from the initial state term. Irrelevant levels are omitted. The radial matrix elements were calculated at each of the energies indicated in Fig. 1, except that we did not examine the cascade from $[2s]^2\,^2P$ to $[2p]^2[3s][3p]$ in Al^{+4} mentioned earlier. The radial matrix elements were calculated by the procedure I have used elsewhere[20]; approximating the central potential of Herman and Skillman[21] by a series of seven straight lines and determining exact discrete and continuum orbitals for the approximate potential. Because there is no relevant data on the Auger spectra of Al and because Coster-Kronig transition rates are sensitive to both the choice of continuum electron energy and the discrete orbitals, I have used the formalism and the matrix-element procedure to calculate the L-shell principal and satellite spectra of argon.[22] The calculations are in excellent agreement with the measurements.[23]

In Table I we list percentage population of terms

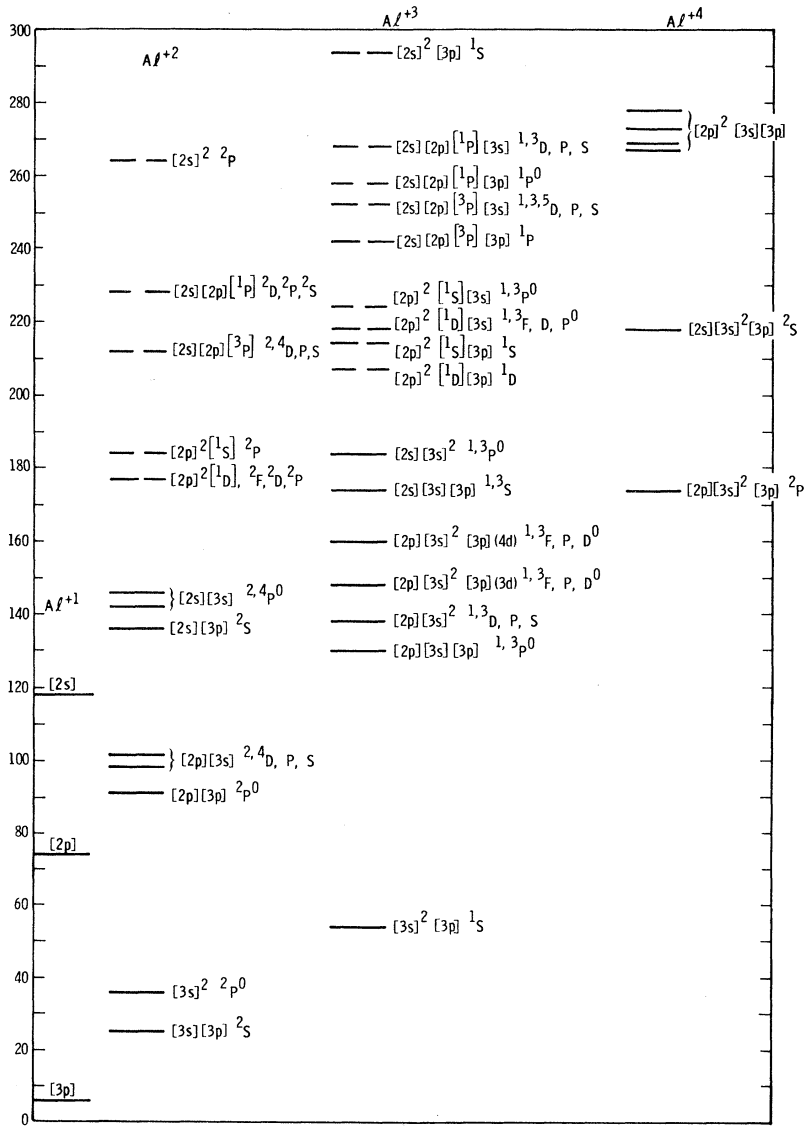

FIG. 1. Energy-level diagram for Al ions. The solid lines indicate level positions based on experiment (Refs. 14, 15, and 16). The dashed lines indicate levels whose positions are estimated as described in the text.

in Al^{+3} arising in the cascade from $[2s]^2\,^2P$ in Al^{+2}. In determining the lifetime of the Al^{+3} terms in this cascade, it was found that, where energetically allowed, S terms would preferentially populate $[2s][3s]^2[3p]^2S$, while all others would go to the $[2p][3s]^2[3p]^2P$ ground state of Al^{+4}. As is seen by the populations in Table I, there is no possibility of an inversion in Al^{+4} via this cascade. Table I further indicates that the $[2s][3s]^2\,^3P, ^1P$ terms have both a large width and an almost negligible fractional population. We would not expect to see much radiation to the $[3s]^2[3p]^1S$ ground state as a result of this cascade. We return to this in Sec. IV.

In Table II we list the percentage population of Al^{+3} terms arising from the decay of the $[2s][2p]$ terms in Al^{+2}. It is seen that there are many terms of the Al^{+3} $[2p]^2[3s]$ and $[2p]^2[3p]$ configurations for which the fractional population is 1–3% and the Auger width is less than 10^{-3} eV. These terms can lead to significant $[2p]^2[3s] \rightarrow [2p][3s]^2$ radiative transitions in the 135–155-Å region, and $[2p]^2[3p] \rightarrow [2p][3s][3p]$ radiative transitions near 160 Å, providing configuration interaction between $[2s]^2[3s]$ and $[2p]^2[3s]$, and $[2s]^2[3p]$ and $[2p]^2[3p]$ does not lead to considerably shorter lifetimes.

In fact, if we start with Al^+ $(1s)^2(2s)^2(2p)^6(3s)^2$, the dominant Auger transition after K-shell ionization is to Al^{+3} $(1s)^2(2s)^2(2p)^4(3s)^2\,^1D$ which has no configuration interaction with $(1s)^2(2s)^0(2p)^6(3s)^2\,^1S$. Fifty-five percent of the K-shell vacancies will cascade to the Al^{+3} $(1s)^2(2s)^2(2p)^4(3s)^2\,^1D$ term. This term has a relatively long Auger lifetime, 0.7×10^{-12} sec. It can radiatively decay to the $(1s)^2(2s)^2(2p)^5(3s)^1P$ term, and the latter can decay, radiatively, to the ground state. This could result in a self-terminating laser system in the 160–165-Å range. The wavelength depends on the precise position of the ^1D term.

In Table II we do not list any decays to the $[2s][3s]^2\,^{1,3}P^0$ terms of Al^{+3}. The transition rate does not vanish identically; rather it is negligibly small. Thus, this cascade will not lead to any significant $(2s)^1(2p)^6(3p) \rightarrow (2s)^2(2p)^6$ radiation.

In Table III we list the percentage population of Al^{+3} terms arising from the decay of the $[2p]^2\,^1D, ^1S$ terms in Al^{+2}. It is clear that the $(2p)^5(3s)^3P$ is the term most heavily populated by the Auger cascade. Thus, the strongest radiative transition in Al^{+3} due to K-shell vacancy production in Al is the $(2p)^5(3s)^3P_1 \rightarrow (2p)^6\,^1S_0$ at 161.7 Å. This transition is spin forbidden but occurs because of the spin-orbit coupling of the $^3P_1$ and $^1P_1$ terms.

As mentioned earlier, in a more sophisticated treatment of the term values in Al^{+2}, one expects some configuration-interaction mixing of $[2s]^2\,^2P$ in the $[2p]^2\,^2P$ terms. The $[2p]^2\,^2P$ terms can then decay to $[2s][3s]^2$ and $[2s][3s][3p]$. The width associated with the $[2s]^2 \rightarrow [2s][3s]^2$ and $[2s]^2 \rightarrow [2s][3s][3p]$ is 0.030 eV. Comparing this with the widths in Table III we see that if $(C_i)^2$ measures the mixture of $[2s]^2\,^2P$ in $[2p]^2\,^2P$ we expect about $\frac{1}{2}(C_i)^2$ of the $[2p]^2\,^2P$ term populations to cascade to $[2s][3s]^2$ and $[2s][3s][3p]$. However, detailed examination of the transition rates involved indicates 90% in $[2s][3s][3p]$ and 10% in $[2s][3s]^2$. Thus, we have a weakly populated $(2s)^1(2p)^6(3p)$ configuration.

Finally, we examine the possibility of lasing at about 165 Å via the $(2p)^4\,^1D(3s)^2\,^1D \rightarrow (2p)^5(3s)^1P$ transition. The radiative transition rate for this is the same as for $(2p)^5(3s)^1P \rightarrow (2p)^6\,^1P$, and is roughly 1.7×10^{10}/sec.[24] Since the Auger decay rate is 1.4×10^{12}/sec, it is clear that this term has a fluorescence yield of 0.01. The gain cross section is then $(1.61\times10^{-7})^2/2\pi \approx 4\times10^{-15}$. Tomboulian and Pell[25] measure a photoionization cross section of about 2×10^{-18} cm^2 at 160 Å in metallic Al. Thus, for net gain we would need to

TABLE I. Initial- and final-state widths and populations in the decay of the $(2s)^0(2p)^6(3s)^2(3p)$ configuration.

Initial state (IS)			$(2s)^0(2p)^6(3s)^2(3p)$	
IS width (eV)			3.50	
IS population (%)			8.25	
Final State (FS)			FS width (eV)	FS population (%)
$[(2s)^1(2p)^5C_1C_3]$				
$[(3s)^1(3p)^1C_2C_4]PQ$				
C_1C_3	C_2C_4	PQ		
^3P	^3P	^3D	0.031	1.06
		^3P	0.031	0.64
		^3S	0.054	0.21
		^1D	0.046	0.53
		^1D	0.046	0.32
		^1S	0.081	0.11
^3P	^1P	^3D	0.008	0.53
		^3P	0.008	0.32
		^3S	0.045	0.11
^1P	^3P	^3D	0.011	1.43
		^3P	0.011	0.86
		^3S	0.023	0.29
^1P	^1P	^1D	0.010	0.48
		^1P	0.010	0.29
		^1S	0.047	0.095
$[(2s)^1(2p)^5(3s)^2]PQ$				
		^3P	0.017	0.060
		^1P	0.016	0.90
$[(2s)^1(2p)^6(3s)]PQ$				
		^3S	1.19	0.003
		^1S	0.25	0.060
$[(2s)^1(2p)^6(3p)]PQ$				
		^3P	0.38	0.004
		^1P	0.39	0.001

TABLE II. Initial- and final-state widths and populations in the decay of the $(2s)^1(2p)^5(3s)^2(3p)$ configuration.

Initial state (IS)			$[(2s)^1(2p)^5D_1L_4][(3s)^2(3p)^1{}^2P]D_3D_6$									
IS			$^3P,{}^4D$	$^3P,{}^4P$	$^3P,{}^4S$	$^3P,{}^2D$	$^3P,{}^2P$	$^3P,{}^2S$	$^1P,{}^2D$	$^1P,{}^2P$	$^1P,{}^2S$	
IS width (eV)			1.19	1.31	1.10	1.33	1.21	1.21	1.45	1.42	1.60	
IS population (%)			2.26	1.34	0.45	1.13	0.68	0.23	11.6	7.0	2.33	
Final state (FS)			FS width (eV)	FS population (%)								Total (%)
$(2s)^1(2p)^6(3s)^1{}^3S$			1.19	•••	•••	•••	•••	•••	0.012	•••	•••	0.042	0.054
	^1S		0.25	•••	•••	•••	•••	•••	0.006	•••	•••	•••	0.006
$[(2p)^4C_1C_3][(3s)(3p)C_2C_4]PQ$													
C_1C_3	C_2C_4	PQ											
^1S	^3P	^3P	0.0044	0.12	0.064	0.026	0.013	0.009	•••	0.615	0.38	0.11	1.34
	^1P	^1P	0.015	•••	•••	•••	0.040	0.026	0.009	0.204	0.13	0.038	0.45
^1D	^3P	^3F	6.0×10^{-5}	0.50	•••	•••	0.056	0.037	•••	2.58	•••	•••	3.18
		^3D	1.6×10^{-5}	0.088	0.24	•••	0.010	0.008	•••	0.46	1.42	•••	2.23
		^3P	0.022	•••	0.080	0.128	•••	•••	0.015	0.030	0.48	0.56	1.30
	^1P	^1F	0.012	•••	•••	•••	0.168	0.110	•••	0.86	•••	•••	1.14
		^1D	0.0031	•••	•••	•••	0.030	0.020	•••	0.15	0.48	•••	0.68
		^1P	0.040	•••	•••	•••	•••	•••	0.045	0.011	0.16	0.19	0.41
^3P	^3P	^5D	•••	0.013	•••	•••	•••	•••	•••	•••	•••	•••	0.013
		^5P	•••	•••	•••	•••	•••	•••	•••	•••	•••	•••	•••
		^5S	•••	•••	•••	•••	•••	•••	•••	•••	•••	•••	•••
		^3D	9.3×10^{-5}	0.61	0.182	•••	0.098	0.065	•••	1.69	0.58	•••	3.23
		^3P	0.027	0.20	0.110	0.175	0.033	0.021	0.029	0.56	0.35	0.41	1.89
		^3S	•••	•••	0.146	•••	•••	0.029	•••	•••	0.46	•••	0.64
		^1D	1.4×10^{-4}	•••	•••	•••	0.324	0.118	•••	0.85	0.29	•••	1.58
		^1P	0.040	•••	•••	•••	0.108	0.071	0.097	0.28	0.17	0.21	0.94
		^1S	•••	•••	•••	•••	•••	0.094	•••	•••	0.23	•••	0.32
^3P	^1P	^3D	0.0092	0.34	0.103	•••	0.016	0.006	•••	0.85	0.29	•••	1.60
		^3P	0.029	0.11	0.062	0.099	0.005	0.003	•••	0.28	0.17	0.21	0.94
		^3S	•••	•••	0.083	•••	•••	0.005	•••	•••	0.23	•••	0.32
$(2p)^4(3s)^2$		^3P	9.5×10^{-4}	0.18	0.213	•••	0.181	0.066	•••	0.012	0.10	•••	0.75
		^1D	9.5×10^{-4}	•••	•••	•••	0.018	•••	•••	1.49	0.91	0.36	2.78
		^1S	9.5×10^{-4}	•••	•••	•••	•••	•••	•••	0.40	•••	0.15	0.55
$(2p)^5(3s)$		^3P	•••	0.038	0.021	0.008	0.013	0.009	•••	•••	•••	•••	0.09
		^1P	•••	•••	•••	•••	•••	•••	•••	0.150	0.09	0.03	0.28
$(2p)^5(3p)$		^3D	•••	0.036	0.019	0.008	•••	•••	•••	0.113	•••	•••	0.18
		^3P	•••	•••	•••	•••	•••	•••	•••	•••	0.07	•••	0.07
		^3S	•••	•••	•••	•••	•••	•••	•••	•••	•••	0.02	0.02
		^1D	•••	•••	•••	•••	0.012	•••	•••	0.039	•••	•••	0.05
		^1P	•••	•••	•••	•••	•••	0.008	•••	•••	0.02	•••	0.03

TABLE III. Initial- and final-state widths and populations in the decay of the $(2p)^4(3s)^2(3p)$ configuration.

Initial state (IS)		$[(2s)^2(2p)^4D_1D_4][(3s)^2(3p)\ ^2P]D_3D_6$				
IS		$^1S, ^2P$	$^1D, ^2F$	$^1D, ^2D$	$^1D, ^2P$	
IS width (eV)		0.010	0.0020	0.000 65	0.045	
IS population (%)		4.20	25.6	18.4	11.1	
Final state (FS)	FS width (eV)	FS population (%)				Total (%)
$(2p)^5(3s)\ ^3P$	•••	4.03	18.6	9.93	10.6	43.1
^1P	•••	0.09	4.62	2.45	0.01	7.17
$(2p)^5(3p)\ ^3D$	•••	0.04	1.96	1.07	0.001	3.07
^3P	•••	0.02	•••	3.52	0.02	3.56
^3S	•••	0.007	•••	•••	0.02	0.027
^1D	•••	0.01	0.64	0.38	0.0003	1.03
^1P	•••	0.007	•••	1.07	0.005	1.08
^1S	•••	0.002	•••	•••	0.007	0.01

ionize the K shell of every thousandth ion of Al^+. A similar scheme occurs in Mg^{+2}, with lasing in the 180–190-Å region. The power level needed can be estimated from the argument that irradiation by a high-power laser of energy Q and pulse duration τ of a converter surface of area S, will lead to the generation of hard x rays. These hard x rays will generate K-shell vacancies in Al^+ and a cascade to the $(2p)^4(3s)^2\ ^1D$ term. Roughly, the population of this level is given by

$$\frac{dN}{dt}=P-\frac{N}{\tau_A},\quad N=P\tau_A(1-e^{-t/\tau_A})=P\tau_A,$$

where τ_A is the Auger lifetime (0.7×10^{-12} sec), and

$$P=\frac{Q}{\tau S}N_0\frac{\sigma_K}{\overline{E}_K}\eta,$$

where N_0 is the Al^+ density, σ_K is the K-shell absorption cross section at some average x-ray flux energy E_K (taken as 10^{-19} cm^2 at 2 keV), and η is a lumped efficiency including conversion of laser photons to x rays, transmission through the converter-filter, and geometrical factors. The criterion for net gain

$$\sigma_g N\gg\sigma_a(165\ \text{Å})N_{\text{tot}},$$

where N_{tot} is the entire Al ion density contributing to absorption at the lasing wavelength (165 Å). We ease this criterion and let $N_{\text{tot}}=N_0$ (the Al^+ density). Then we have

$$\frac{\eta Q}{\tau S}N_0\frac{\sigma_K}{\overline{E}_K}\tau_A\frac{\lambda^2}{2\pi}\frac{\tau_A}{\tau_R}\gg2\times10^{-18}N_0,$$

where τ_R is the radiative lifetime (0.6×10^{-10} sec). This leads to

$$\frac{\eta Q}{\tau S}\gg2\times10^{-18}\frac{\overline{E}_K}{\sigma_K}\frac{\tau_R}{(\tau_A)^2}\frac{2\pi}{\lambda^2}=2\times10^{11}\ \text{J/cm}^2\,\text{sec}.$$

This is effectively an x-ray flux, while the necessary laser flux is $2\times10^{11}/\eta$ (J/cm^2 sec) $\approx10^{13}$–10^{14} J/cm^2 sec, for $\eta=10^{-2}$–10^{-3}. Such flux levels are attainable with state-of-the-art high-power glass laser systems. This is assuming $N_{\text{tot}}=N_0$. However, this is a self-terminating system. There is a possible four-level system [i.e., a similar calculation can be made for the $(2p)^4\ ^1D(3s)^2(3p)^2D \rightarrow(2p)^5(3s)(3p)$ transition complex in Al^{+2}]. The calculated Auger lifetime of the initial term is 10^{-12} sec. The advantages in this transition are that the lower level should not be populated by plasma recombination effects, and that the lower level will Auger decay. A disadvantage is that the lower level can be populated by $[2s]$-$[2p][3s]$ Auger transitions and $[2s]$ vacancies can be created by photoelectrons. Another disadvantage is the low branching ratio of 0.18 as opposed to 0.55 in the preceding example.

In determining the minimum flux level for amplified spontaneous emission above, I used the natural linewidth determined by the Auger lifetime as the total linewidth. In a solid this requires ion and electron densities of about 10^{20}/cm^3. Alternative broadening mechanism may be important at these densities. The estimates of McCorkle and Joyce[26] indicate that electron impact broadening can lead to a width a factor of 10 larger than the one used above. If experiment shows the estimates of McCorkle and Joyce[26] are accurate and $\Delta\nu\approx4\times10^{12}$ Hz, then amplified spontaneous emission from solid Al with present-day glass lasers would require a factor of 10 increase in x-ray conversion efficiency η. However, in an Al vapor, the Auger widths will not change, while the alternate broadening mechanisms will be substantially decreased. Doppler broadening would not be significant if the ion temperature were less than 10 eV.

IV. RELEVANCE TO EXPERIMENT

As mentioned in Sec. I, Valero[11] has reported that the observations of Jaegle *et al.*[10] can be accounted for by selective self-absorption. Recently, Jaegle *et al.*[27] have reported the appearance of gain in a two-plasma Al system in the $(2p)^5(4d)\,^3P_1 \rightarrow (2p)^6\,^1S_0$ transition in Al^{+3}. Jaegle *et al.* measure the emission of the two plasmas separately, I_1 and I_2, and jointly I and find that $T=(I-I_2)/I_1$ can be greater than unity, indicating gain. However, if the $(2p)^5(4d)\,^3P_1$ population has a significant contribution from Auger cascades following K-shell ionization of neutral Al, then the absorption of hard x rays from the first plasma by the second plasma could account for $I>I_1+I_2$. Some indication that this may occur is found in the argon L-MM Auger spectra[22,23] where there appears to be a significant configuration interaction between the $(3s)(3p)^5$ and $(3s)^2(3p)^3(3d)$ configurations. Then one would expect a weaker configuration interaction between $(3s)(3p)^5$ and $(3s)^2(3p)^3(nd)$ $(n=4, 5\ldots)$. Table III indicates that 43% of all K-shell vacancies in Al cascade to the $(2p)^5(3s)\,^3P$ term. Configuration interaction between this term and $(2p)^5(nd)\,^3P$ can populate the initial term in the transition observed by Jaegle *et al.*[27] Quantitative calculations on this hypothesis do not appear feasible, but the above considerations suggest an experimental check of the hypothesis. That is, $I>I_1+I_2$ for the $(2p)^5(3s)\,^3P \rightarrow (2p)^6$ transition at 162 Å. In following the Auger cascades in Sec. III, it was shown that there would be negligible radiation emitted in the $(2s)^1(2p)^6(3p) \rightarrow (2s)^2(2p)^6$ transition. This is consistent with the observation of Valero.[11]

V. CONCLUSIONS

Applying the transition rate expressions for Auger cascades to Al, we have found levels with sufficient population inversion following K-shell vacancy production to produce amplified spontaneous emission. The K-shell vacancy production rate requires incident laser pump fluxes of 10^{13}–10^{14} W/cm^2. The high electron and ion densities generated in a solid could lead to broadening significantly greater than that due to the Auger width. If this is the case, Al vapor could be used as the medium for amplified spontaneous emission. A hypothesis was introduced that the appearance of gain in the two plasma experiment of Jaegle *et al.* could be accounted for via x-ray coupling between the plasmas, and an experimental check of this hypothesis was suggested. In general, this work suggests that large inner-shell population inversions can be produced via the Auger effect, and that calculations can estimate both the size of the inversion and the wavelength at which one might expect amplified stimulated emission.

---

*This work supported by U.S. Energy Research and Development Administration.

[1]K. D. Sevier, *Low Energy Electron Spectrometry* (Wiley-Interscience, New York, 1972).
[2]E. H. S. Burhop and W. N. Asaad, in *Advances in Atomic and Molecular Physics* (Academic, New York, 1973), Vol. 8.
[3]E. J. McGuire, in *Atomic Inner-Shell Processes*, edited by B. Crasemann (Academic, New York, 1975).
[4]W. Bambynek, B. Crasemann, R. W. Fink, H. U. Freund, H. Mark, C. D. Swift, R. E. Price, and P. Venugopala Rao, Rev. Mod. Phys. 44, 716 (1972).
[5]G. N. Ogurtsov, Rev. Mod. Phys. 44, 1 (1972).
[6]M. O. Krause and T. A. Carlson, Phys. Rev. 158, 18 (1967).
[7]E. J. McGuire, Phys. Rev. A 10, 32 (1974).
[8]E. J. McGuire, Phys. Rev. A 10, 13 (1974).
[9]E. J. McGuire (unpublished).
[10]P. Jaegle, A. Carillon, P. Dhez, G. Jamelot, A. Sureau, and M. Cukier, Phys. Lett. 36A, 167 (1971).
[11]F. P. J. Valero, Appl. Phys. Lett. 25, 64 (1974).
[12]L. C. Biedenharn, J. Math. and Phys. 31, 289 (1953); J. P. Elliott, Proc. R. Soc. Lond. A218, 345 (1953).
[13]A. P. Yutsis, I. B. Levinson, and V. V. Vanagas, *Theory of Angular Momentum* (National Science Foundation, Washington, D.C., 1960).
[14]K. Siegbahn *et al.*, in *ESCA, Atomic, Molecular and Solid State Structure Studied by Means of Electron Spectroscopy* (Nova Acta Ragiae Societatis Upsaliensis, Uppsala, 1967), Ser. IV, Vol. 20.
[15]C. E. Moore, *Atomic Energy Levels*, NBS Circ. No. 467 (U.S. GPO, Washington, D.C., 1957).
[16]R. Abouaf, Phys. Lett. 35A, 319 (1971).
[17]F. P. Larkins, in *Proceedings of the International Conference on Inner-Shell Ionization Phenomena and Future Applications, Atlanta, Georgia, 1972*, edited by R. W. Fink, S. T. Manson, I. M. Palms, and P. V. Rao, CONF-720 404 (U.S. Atomic Energy Commission, Oak Ridge, Tenn., 1973), p. 2193.
[18]D. A. Shirley, Phys. Rev. A 7, 1520 (1973).
[19]W. N. Asaad, Nucl. Phys. 66, 494 (1965).
[20]E. J. McGuire, Phys. Rev. A 2, 273 (1970); 3, 587 (1971); 5, 1043 (1972); 9, 1840 (1974).
[21]F. Herman and S. Skillman, *Atomic Structure Calculations* (Prentice-Hall, Englewood Cliffs, N.J., 1963).
[22]E. J. McGuire, preceding paper, Phys. Rev. A 11, 1880 (1975).
[23]L. O. Werme, T. Bergmark, and K. Siegbahn, Physica Scripta 8, 149 (1973).
[24]W. L. Wiese, M. W. Smith, and B. M. Miles, *Atomic Transition Probabilities*, U.S. Natl. Bur. Stand. Ref. Data Ser. No. 22 (U.S. GPO, Washington, D.C., 1969), Vol. II.
[25]D. H. Tomboulian and E. M. Pell, Phys. Rev. 83, 1196 (1951).
[26]R. A. McCorkle and J. M. Joyce, Phys. Rev. A 10, 903 (1974).
[27]P. Jaegle, G. Jamelot, A. Carillon, A. Sureau, and P. Dhez, Phys. Rev. Lett. 33, 1070 (1974).